

Solitary States and Partial Synchrony in Oscillatory Ensembles with Attractive and Repulsive Interactions

Erik Teichmann^{1, a)} and Michael Rosenblum^{1, 2}

¹⁾*Institute of Physics and Astronomy, University of Potsdam, Karl-Liebknecht-Str. 24/25, 14476 Potsdam-Golm, Germany*

²⁾*Control Theory Department, Institute of Information Technologies, Mathematics and Mechanics, Lobachevsky University Nizhny Novgorod, Russia*

(Dated: 8 July 2019)

We numerically and analytically analyze transitions between different synchronous states in a network of globally coupled phase oscillators with attractive and repulsive interactions. The elements within the attractive or repulsive group are identical, but natural frequencies of the groups differ. In addition to a synchronous two-cluster state, the system exhibits a solitary state, when a single oscillator leaves the cluster of repulsive elements, as well as partially synchronous quasiperiodic dynamics. We demonstrate how the transitions between these states occur when the repulsion starts to prevail over attraction.

PACS numbers: 05.45.Xt Synchronization; coupled oscillators

Networks of coupled oscillators are a popular model for many engineered or natural systems. The main effect – emergence of a collective mode via synchronization – is now well-understood and therefore focus of research shifted recently to analysis of different complex states. These states include chimeras, when a population of identical units splits into a synchronous and asynchronous part, quasiperiodic partially synchronous states, characterized by the difference of frequencies of individual units and of the collective mode, and clusters and heteroclinic cycles, to name just a few. Of particular interest are ensembles where some elements have only attractive connections while others have only repulsive ones. This model is motivated by studies of neuronal networks that are built from excitatory and inhibitory neurons. In this paper we analyze how the state of such a setup changes with the interplay of attraction and repulsion. We demonstrate that if the frequency mismatch between attractive and repulsive units is smaller than some critical value then desynchronization occurs via appearance of the solitary state. With the further increase of repulsion the system undergoes a transition to quasiperiodic partial synchrony. In the latter state the attractive units remain synchronized, while the repulsive group settles between synchrony and asynchrony so that the mean fields of both groups remain locked, but the frequency of the repulsive elements is larger than that of their mean field. For a large frequency mismatch of attractive and repulsive groups desynchronization immediately leads to partial synchrony.

I. INTRODUCTION

Investigation of coordinated dynamics of many interactive oscillatory elements is relevant for the understanding of various phenomena from different branches of science. Probably, the most important and also mostly studied effect is the emergence of a collective mode, observed in populations of flashing fireflies¹, groups of pedestrians on footbridges² or metronomes placed on a common support³, electronic circuits⁴, populations of cells⁵, synthetic genetic oscillators⁶, etc. Besides of collective synchrony, oscillatory networks exhibit many other interesting dynamical states like clusters and heteroclinic switching⁷, chimeras⁸, collective chaos⁹, traveling waves¹⁰, quasiperiodic partial synchrony^{11–14}, solitary states¹⁵, and so on. Analysis of such states and transitions between them is in the focus of current research.

Some of mentioned effects can be studied within the framework of the famous Kuramoto model¹⁶ and of its immediate extension, the Kuramoto-Sakaguchi model¹⁷, that treat phase oscillators with the sine-coupling. Though this is a rather simplistic description of real-world oscillators, these models became extremely popular due to the possibility of analytical treatment^{18,19}. For example, they allow for theoretical description of synchronization transitions (that, in dependence on the distribution of oscillatory frequencies, can be alike second- or first-order²⁰ phase transitions). Due to their specific mathematical properties, sine-coupled phase oscillators also often admit a low-dimensional description via the Watanabe-Strogatz (WS)^{4,21} and Ott-Antonsen (OA)^{22,23} theories. All this explains

^{a)}Electronic mail: kontakt.teichmann@gmail.com

why the Kuramoto-Sakaguchi model became a paradigmatic one, with applications ranging from explanation of social effects^{1,2} to neuroscience²⁴.

In most variants of the Kuramoto-Sakaguchi model researchers treat networks with attractive interactions and the existing literature extensively covers this case^{25–27}. Networks of repulsive elements attract much less attention, although they show interesting effects^{28–30}. Not much attention is also paid to mixed networks^{31–36}, consisting of both attractive and repulsive elements, though systems of this type are common in neuroscience, because real neurons interact via excitatory and inhibitory connections^{37–40}.

In this paper we concentrate on emergence of solitary state and quasiperiodic partial synchrony in networks with attractive and repulsive connections. The solitary state, when a single repulsive unit leaves the synchronous cluster, was for the first time found and analyzed in Ref.¹⁵ and later in Refs.^{41–45}. A generalized solitary state, where several oscillators exhibit dynamics different from that of the synchronous cluster received attention in Refs.^{46–55}. This state appears at the border between synchrony and asynchrony, as soon as repulsion starts to prevail over attraction. Our setup is an extension of the finite-size two-group Kuramoto model treated in Ref.¹⁵, where all oscillators were identical.

We demonstrate that for small frequency mismatches between the groups and a weak repulsion, there appears a small region, where the attractive units build a synchronous cluster, while the repulsive oscillators exhibit quasiperiodic partially synchronous dynamics. Slightly stronger repulsion leads to the solitary state, which is replaced by quasiperiodic dynamics again for bigger repulsion. For large mismatches in the frequency the solitary state is not observed, but only quasiperiodic dynamics.

II. THE MODEL

A popular version of the standard Kuramoto-Sakaguchi model is a system of M interacting groups of identical units, described by the following equations:

$$\dot{\theta}_j^\sigma = \omega_\sigma + \sum_{\sigma'=1}^M \frac{K_{\sigma\sigma'}}{N} \sum_{k=1}^{N_{\sigma'}} \sin(\theta_k^{\sigma'} - \theta_j^\sigma + \alpha_{\sigma\sigma'}), \quad (1)$$

where θ_j^σ is the phase of the i th oscillator in the group σ and $\sigma = 1, \dots, M$. Here ω_σ and N_σ are the natural frequency and the number of oscillators in the group σ , $N = \sum_\sigma N_\sigma$, and $K_{\sigma\sigma'}$ and $\alpha_{\sigma\sigma'}$ are respectively the strength of the coupling and the phase shift characterizing interaction between groups σ and σ' .

In the following we analyze a two-group Kuramoto-Sakaguchi model wherein the coupling coefficients and the phase shift parameters depend on the acting group only, i.e. $K_{\sigma\sigma'} = K_{\sigma'}$ and $\alpha_{\sigma\sigma'} = \alpha_{\sigma'}$. We concentrate on a particular case, motivated by neuroscience applications, when the coupling within the first group is attractive while in the second group it is repulsive. We denote phases of the units in these groups by φ and ψ , respectively. By re-scaling the time and performing a transformation to a reference frame co-rotating with the frequency of the attractive group, we write the model as

$$\begin{aligned} \dot{\varphi}_j &= \frac{1}{N} \sum_{k=1}^{N_a} \sin(\varphi_k - \varphi_j + \alpha_a) - \frac{1+\varepsilon}{N} \sum_{k=1}^{N_r} \sin(\psi_k - \varphi_j + \alpha_r), \\ \dot{\psi}_j &= \omega + \frac{1}{N} \sum_{k=1}^{N_a} \sin(\varphi_k - \psi_j + \alpha_a) - \frac{1+\varepsilon}{N} \sum_{k=1}^{N_r} \sin(\psi_k - \psi_j + \alpha_r), \end{aligned} \quad (2)$$

where subscripts a and r stand for “attractive” and “repulsive”, respectively. Quantification of coupling has been reduced to a single parameter $K_r/K_a = -(1+\varepsilon)$, with ε being the excess of repulsive coupling. An $\varepsilon < -1$ indicates that interaction within both groups is attractive and, trivially, the whole system synchronizes. For $\varepsilon = -1$ the second group is uncoupled and in the range $-1 < \varepsilon < 0$ the repulsive coupling is weaker than the attractive coupling. For $\varepsilon = 0$ their magnitudes are identical and for $\varepsilon > 0$ the repulsive coupling dominates.

Introducing the Kuramoto mean fields for both groups, $Z_a = \rho_a e^{i\Theta_a} = 1/N_a \sum e^{i\varphi_j}$, $Z_r = \rho_r e^{i\Theta_r} = 1/N_r \sum e^{i\psi_j}$, and the common forcing

$$H = h e^{i\Phi} = \frac{N_a}{N} e^{i\alpha_a} Z_a - \frac{N_r}{N} (1+\varepsilon) e^{i\alpha_r} Z_r, \quad (3)$$

we re-write the model in a compact form as

$$\dot{\varphi}_j = \text{Im} [H e^{-i\varphi_j}] = h \sin(\Phi - \varphi_j), \quad (4)$$

$$\dot{\psi}_j = \omega + \text{Im} [H e^{-i\psi_j}] = \omega + h \sin(\Phi - \psi_j). \quad (5)$$

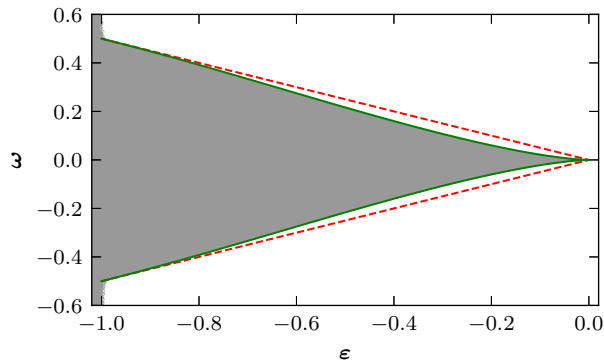


FIG. 1. Full synchrony in system (4,5) is a two-cluster state. The region of full synchrony, as obtained numerically, is shaded with gray, while all other states are shown with white. The dashed red and the solid green lines show the analytical results for boundary of existence and of stability of the two-cluster state, respectively, see Eqs. (9,15).

For the further analysis we restrict ourselves to the case of equally sized groups $N_r = N_a = N/2$ and $\alpha_a = \alpha_r = 0$. Equation (3) then reduces to

$$H = h e^{i\Phi} = \frac{1}{2} [Z_a - (1 + \varepsilon)Z_r]. \quad (6)$$

We notice that according to the Watanabe-Strogatz (WS) theory^{4,21} the dynamical description of $n > 3$ identical oscillators subject to a common force can be reduced to equations for three global variables and $n - 3$ constants of motion. Thus, for $N_{a,r} > 3$ and $\omega \neq 0$ the model (4,5) is in fact 6-dimensional and can be described by two coupled systems of WS equations, see Ref.⁵⁶. For $\omega = 0$ all oscillators become identical and the whole ensemble can be described by three WS equations.

III. SYNCHRONOUS STATE

First we analyze conditions of existence and stability of a synchronous state, where $\varphi_j = \varphi$ and $\psi_j = \psi$ for all j and observed frequencies are $\dot{\varphi} = \dot{\psi} = \nu$. Notice that generally $\varphi \neq \psi$, i.e. synchrony in this setup shall be understood as existence of a two-cluster state. Notice also that for $\varepsilon < -1$ both groups are attractive and synchronize regardless of ω , therefore we are interested in the interval $\varepsilon > -1$. Let $\varphi = \nu t$, $\psi = \nu t + \psi_0$, and $\Phi = \nu t + \Phi_0$. Then real and imaginary parts of Eq. (6) provide

$$\begin{aligned} h \cos \Phi_0 &= \frac{1}{2} - \frac{1 + \varepsilon}{2} \cos \psi_0, \\ h \sin \Phi_0 &= -\frac{1 + \varepsilon}{2} \sin \psi_0. \end{aligned} \quad (7)$$

a. Condition of existence. Subtracting Eq. (4) from Eq. (5) and using $\dot{\psi}_0 = 0$ we find that

$$\omega = h[\sin \Phi_0 - \sin(\Phi_0 - \psi_0)]. \quad (8)$$

Writing the second term as $\sin \Phi_0 \cos \psi_0 - \cos \Phi_0 \sin \psi_0$ and excluding $\sin \Phi_0$ and $\cos \Phi_0$ using Eqs. (7) we obtain

$$\sin \psi_0 = -\frac{2\omega}{\varepsilon}. \quad (9)$$

It follows, that synchrony does not exist for $\varepsilon = 0$, when attraction and repulsion are balanced. For $\varepsilon > 0$ the repulsion becomes stronger than attraction and therefore the synchronous two-cluster state cannot be expected either. This consideration yields the border of the synchronous domain for $\varepsilon < 0$:

$$|\omega| \leq -\varepsilon/2. \quad (10)$$

In order to find the observed frequency ν we expand (5) and insert (7). Together with (9) this yields

$$\nu = \frac{1 + \varepsilon}{\varepsilon} \omega . \quad (11)$$

Notice that the ratio $(1 + \varepsilon)/\varepsilon$ is negative in the region of existence, so that two synchronous clusters rotate in the direction, opposite to the one determined by ω . (We remind that we consider the motion in a frame, co-rotating with the natural frequency of the attractive group.)

b. Condition of stability. The next step is to determine stability of the two-cluster configuration. For this purpose we first consider the linear stability of the repulsive cluster with respect to a symmetric perturbation⁵⁷. It means that phases of two perturbed oscillators become $\psi_{\pm} = \nu t + \psi_0 \pm \alpha$, where $\alpha \ll 1$. This assures that the mean field Z_r remains unchanged in the first-order approximation in α . The perturbed oscillators then evolve according to

$$\dot{\psi}_{\pm} = \omega + h \sin(\Phi_0 - \psi_0 \mp \alpha) . \quad (12)$$

In the first order in α we find

$$\dot{\alpha} = -\alpha h \cos(\Phi_0 - \psi_0) . \quad (13)$$

Thus, the cluster is stable for $h \cos(\Phi_0 - \psi_0) > 0$. With the help of Eqs. (7) this condition can be re-written as

$$\cos \psi_0 - (1 + \varepsilon) > 0 . \quad (14)$$

Hence, the border of stability is determined by the condition $\cos \psi_0 = 1 + \varepsilon$. Now, using Eq. (9), we exclude ψ_0 and obtain the stability boundary as

$$\omega = \pm \sqrt{-\frac{\varepsilon^3}{2} - \frac{\varepsilon^4}{4}} . \quad (15)$$

Using the same approach for the attractive group we find the condition for the stability to be

$$\cos \psi_0 < \frac{1}{1 + \varepsilon} . \quad (16)$$

In the domain where the synchronous state exists we have $\varepsilon < 0$ and the latter condition is fulfilled.

Next, we have to consider the stability of the two-cluster configuration with respect to a shift of one of the clusters. For this purpose we re-write Eqs. (4,5) for the special case of $\varphi_j = \varphi$ and $\psi_j = \psi$. Using Eq. (3) we obtain

$$\dot{\varphi} = -\frac{1 + \varepsilon}{2} \sin(\psi - \varphi) , \quad (17)$$

$$\dot{\psi} = \omega - \frac{1}{2} \sin(\psi - \varphi) , \quad (18)$$

which yields the Adler equation⁵⁸ for the distance between the clusters $\delta = \psi - \varphi$:

$$\dot{\delta} = \omega + \frac{\varepsilon}{2} \sin \delta . \quad (19)$$

This equation has a stable fixed point for $|\omega| < -\frac{\varepsilon}{2}$, i.e. in the whole domain of existence of the two-cluster solution.

The final conclusion is that the stability of the synchronous two-cluster state is given by Eq. (15). This result fits very well the numerical results shown in Fig. 1. As one can see, the stable domain is smaller than the region where full synchrony exists.

IV. NONTRIVIAL STATES BEYOND THE TWO-CLUSTER SYNCHRONY

A. Solitary State

The next solution we observe is the three-cluster state. As has been shown in Ref.¹⁵, the system (4,5) with $\omega = 0$, exhibits, beyond the fully synchronous one-cluster solution, a peculiar solitary state, where a cluster of N_a attractive and $N_r - 1$ repulsive oscillators coexists with a phase-shifted solitary oscillator. This state is not of full measure, so that not every initial condition leads to it. The range of the coupling values, where this solution exists shrinks as $1/N$ for $N \rightarrow \infty$. This makes the solitary state reliably observable only for small system sizes. The picture we observe for $\omega \neq 0$ is slightly different. Though the loss of synchrony here also occurs via appearance of a solitary unit, now one finds a three-cluster state: a cluster of N_a attractive oscillators, a cluster of $N_r - 1$ repulsive oscillators, and a solitary repulsive unit. The phase shifts between clusters are constant, so that the whole configuration rotates with the same constant observed frequency ν . An illustration of this can be found in Fig. 2.

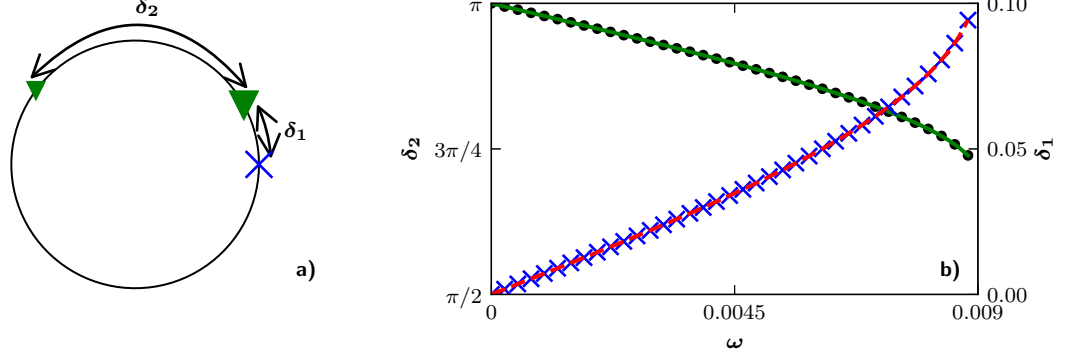


FIG. 2. a) Schematic illustration of the solitary state. Here the big and small green triangles denote the cluster of $N_r - 1$ repulsive units and solitary repulsive oscillator, respectively. The cluster of attractive units is shown by the blue cross. Panel b) shows phase differences $\delta_{1,2}$ in the solitary state for a particular case $N_r = N_a = 5$ and $\varepsilon = 0.212$ (this value corresponds to the largest range of ω for which the solitary state exists, cf. Fig. 3). Here black circles and blue crosses show the results of direct numerical simulation for δ_2 and δ_1 , respectively, while the solid green and the dashed red lines are the theoretical results obtained with the help of Eqs. (26,31). The boundary of the solitary state is at $\omega \approx 0.009$.

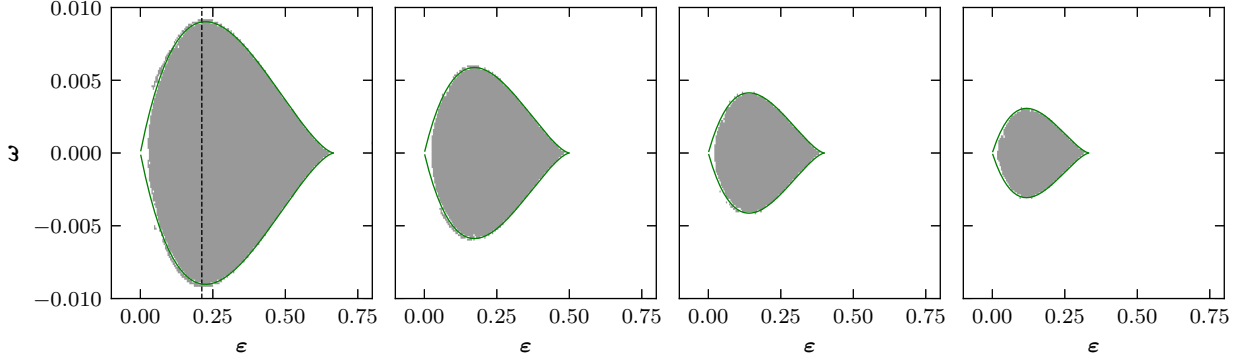


FIG. 3. The solitary state is a state with three clusters of size N_a , $N_r - 1$, and 1, respectively. Parameters where such a state was observed numerically are shaded gray, while all others are shaded white. The solid green line gives the analytically derived boundary, see Eq. (26). The dashed black line in the left panel marks $\varepsilon = 0.212$; this value approximately corresponds to the largest interval of ω where the solitary state exists. The panels from left to right show the results for $N_a = N_r = 5, 6, 7$ and 8.

a. Condition of existence. For a description of this state we write $\varphi = \nu t$, $\psi_{1,\dots,N_r-1} = \nu t + \delta_1$, $\psi_{N_r} = \nu t + \delta_1 + \delta_2$, and $\Phi = \nu t + \Phi_0$. This yields the equations

$$he^{i\Phi_0} = \frac{1}{2} - \frac{1+\varepsilon}{2N_r} \left[(N_r - 1)e^{i\delta_1} + e^{i(\delta_1+\delta_2)} \right], \quad (20)$$

$$\nu = h\text{Im}[e^{i\Phi_0}], \quad (21)$$

$$\nu = \omega + h\text{Im}[e^{i(\Phi_0-\delta_1)}], \quad (22)$$

$$\nu = \omega + h\text{Im}[e^{i(\Phi_0-\delta_1-\delta_2)}]. \quad (23)$$

From the last two equations it follows that $\text{Im}[e^{i(\Phi_0-\delta_1)}] = \text{Im}[e^{i(\Phi_0-\delta_1-\delta_2)}]$ and $\text{Re}[e^{i(\Phi_0-\delta_1)}] = -\text{Re}[e^{i(\Phi_0-\delta_1-\delta_2)}]$. This yields $2\delta_1 + \delta_2 = 2\Phi_0 - \pi$. Multiplying (20) with $e^{-i\Phi_0}$ and taking the imaginary part we find, by replacing h with Eq. (21),

$$\text{Im}[e^{i(\Phi_0-\delta_1)}] = \frac{1}{1+\varepsilon} \text{Im}(e^{i\Phi_0}). \quad (24)$$

By applying this relation to Eqs. (21,22) we find that observed frequency ν is described by the same Eq. (11) as in the synchronous state. However, while in the case of full synchrony $(1+\varepsilon)/\varepsilon$ was negative, here it is positive. Next,

multiplying Eq. (20) by $e^{-i\Phi_0}$ and taking this time the real part we obtain, after replacing $\text{Re}(e^{i\Phi_0}) = \sqrt{1 - \text{Im}(e^{i\Phi_0})^2}$:

$$h = \frac{1}{2} \sqrt{1 - \text{Im}(e^{i\Phi_0})^2} - \frac{N_r - 2}{2N_r} \sqrt{(1 + \varepsilon)^2 - \text{Im}(e^{i\Phi_0})^2}. \quad (25)$$

Finally, replacing h with the help of Eqs. (21,11) and introducing $x = \text{Im}(e^{i\Phi_0})$, we obtain

$$0 = x\sqrt{1 - x^2} - \frac{N_r - 2}{N_r} x\sqrt{(1 + \varepsilon)^2 - x^2} - 2\frac{1 + \varepsilon}{\varepsilon} \omega. \quad (26)$$

To find the parameter domain of existence of the solitary state we need to find the range of ω so that Eq. (26) can be fulfilled for a given ε . First of all notice that Eq. (26) is invariant with respect to the transformation $x \rightarrow -x$ and $\omega \rightarrow -\omega$. The branch for $\omega > 0$ is given by the solution for $x \in (0, 1]$ and the other one can be inferred by using the transformation $\omega \rightarrow -\omega$. Consider the function f consisting of the first two terms on the right hand side of Eq. (26):

$$f(x, N_r, \varepsilon) = x\sqrt{1 - x^2} - \frac{N_r - 2}{N_r} x\sqrt{(1 + \varepsilon)^2 - x^2}. \quad (27)$$

The border of the solitary state for $\omega > 0$ can then be calculated as $\omega = \frac{\varepsilon}{2(1 + \varepsilon)} f_{\max}(x, N_r, \varepsilon)$. To find the maximum of f we write $\partial f / \partial x = 0$, which yields

$$(1 - 2x^2)N_r\sqrt{(1 + \varepsilon)^2 - x^2} = [(1 + \varepsilon)^2 - 2x^2](N_r - 2)\sqrt{1 - x^2}. \quad (28)$$

Squaring Eq. (28) and ordering it by powers of x we get a cubic equation for x^2 . The expression for the roots is too long to be shown here, but the calculated maximal ω for the solitary state fits the numerical results nicely, as shown in Fig. 3.

b. Phase shifts in the solitary state. To determine the phase shifts δ_1 and δ_2 , we first rewrite Eq. (2) in terms of δ_1 and δ_2 :

$$\dot{\delta}_2 = \frac{1}{2} [\sin \delta_2 ((1 + \varepsilon) - \cos \delta_1) - \cos \delta_2 \sin \delta_1 + \sin \delta_1]. \quad (29)$$

Next, similarly to the case of $\omega = 0$ studied in Ref.¹⁵, we write it as

$$\dot{\delta}_2 = A [\sin(\delta_2 - \delta_2^*) + \sin \delta_2^*], \quad (30)$$

where $\tan \delta_2^* = \sin \delta_1 / ((1 + \varepsilon) - \cos \delta_1)$ and $A = \sin \delta_1 / (2 \sin \delta_2^*)$. A stable state has the solution $\delta_2 = 0$ or $\delta_2 = 2\delta_2^* + \pi$. The first solution corresponds to the 2-cluster state and the second solution to the solitary state. As shown earlier the phase shifts in the solitary state are related via $2\Phi_0 - \pi = 2\delta_1 + \delta_2$. This can also be expressed as $\Phi_0 = \delta_1 + \delta_2^*$. Equation (24) then allows one to write the relation between δ_2^* and Φ_0 as

$$\sin \delta_2^* = \frac{1}{1 + \varepsilon} \sin \Phi_0, \quad (31)$$

and consequently allows for the calculation of δ_2 and δ_1 from Φ_0 . Φ_0 can be calculated numerically from Eq. (26) and the resulting phase shifts coincide with the numerical results in Fig. 2.

c. Stability. An analytical linear stability analysis shows that the value of δ_2 is stable in the region of existence. Finding the stability for δ_1 is not as simple and can only be done numerically. Still we find it to be stable in the whole region of existence for $N_a = N_r = 5$. The stability analysis can be found in Appendix A.

d. Case $\omega = 0$ vs. case $\omega \neq 0$. Our numerical results indicate that for $\omega \neq 0$ in the parameter range where the solitary state exists, it is the only attractor. This is an essential difference with the previously studied case $\omega = 0$, see Ref.¹⁵, where the solitary state has not full measure. Indeed, for $\omega = 0$ the system (4,5,6) admits splay state solutions $h = 0$ with $\Theta_a = \Theta_r = \Phi$ and

$$\rho_r = \rho_a / (1 + \varepsilon). \quad (32)$$

For $\omega \neq 0$ the state $h = 0$ is not a solution and numerical studies indicate that the completely asynchronous case $\rho_a = \rho_r = h = 0$ is unstable. Thus, the solitary state remains the only attractor.

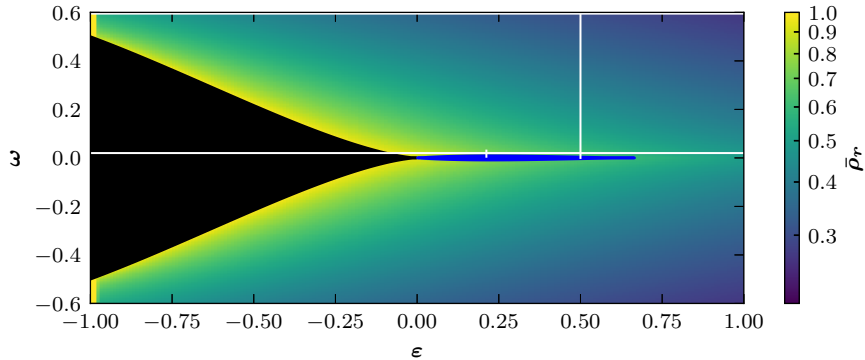


FIG. 4. Overview of the states in the parameter space for $N_a = N_r = 5$. The black region corresponds to the domain of full synchrony as determined by Eq. (15). The blue color shows the domain of solitary states, see Eq. (26). The background outside of these two regions shows the time-averaged order parameter $\bar{\rho}_r$ of the repulsive group for one initial condition; here it is $\bar{\rho}_r < 1$, so that this is the domain of partial synchrony. White lines show parameter values where the dynamics is analyzed in details, see Figs. 6,9.

e. Absence of other clustered states. According to the WS theory^{4,21,59}, the repulsive group can be fully described by two global angle variables Ψ and Γ , global variable $0 \leq \kappa \leq 1$, and N_r constants χ_k , $k = 1, \dots, N_r$. The latter depend on initial conditions and obey three additional constraints. The original phase variables can be obtained from the global ones with the help of the Möbius transformation^{19,60} as $e^{i\psi_k} = e^{i\Gamma}(\kappa + e^{i(\chi_k - \Psi)})/(\kappa e^{i(\chi_k - \Psi)} + 1)$. For $\kappa < 1$, general initial conditions, i.e. different χ_k , yield different ψ_k (for an example of such dynamics see the partially synchronous state described in the next Section). For $\kappa = 1$ typically all $\psi_k = \psi$, i.e. one observes a one-cluster state. However, it is possible that $e^{i(\chi_k - \Psi)} = -1$ for some $k = n$ and then one phase ψ_n differs from other clustered phases, i.e. the solitary state is observed^{15,61}. Other cluster states except for full synchrony and the $(N_r - 1, 1)$ configuration are therefore not allowed, see Ref.⁶² for a rigorous proof. Certainly, similar consideration can be applied to the attractive group, but there the solitary state is unstable and only the trivial one-cluster state is observed.

B. Self-Consistent Partial Synchronization

1. Numerical analysis

Outside of the domains of full synchrony and solitary states we find a partially synchronized repulsive group, characterized by the order parameter $0 < \rho_r < 1$. As for the attractive group, we find that it remains synchronous even for such large values of ϵ as 10. Though the condition of its full synchrony (16) can be easily extended for the general case of $\rho_r \leq 1$ to $\rho_r \cos(\Theta_r - \Theta_a) < (1 + \epsilon)^{-1}$, we were not able to prove the synchrony analytically and only checked it numerically⁶³. A diagram of the states, including the domains of existence of full synchrony and of the solitary state, combined with the presentation of the time-averaged order parameter $\bar{\rho}_r$ ⁶⁴ can be found in Fig. 4.

The observed partial synchrony can be seen as a self-organized quasiperiodic state, SOQ (or self-consistent partial synchrony, SCPS)¹²⁻¹⁴. The latter is characterized by the difference between the average frequency of the oscillators and their mean field. Indeed, in our setup the average frequency (observed frequency) $\bar{\nu}_r$ of repulsive units is larger than the average frequency $\bar{\Omega}_r$ of their mean field. (In fact, the instantaneous frequencies also differ nearly all the time.) Furthermore, the mismatch $\bar{\nu} - \bar{\Omega}_r$ increases with ω . Nevertheless, both sub-populations remain synchronous on the macroscopic level, i.e. the average mean field frequencies coincide, $\bar{\Omega}_r = \bar{\Omega}_a$, see Fig. 5. We notice that close to the border of the solitary state these frequencies are not always well-defined, as indicated by small values of the minimal instantaneous order parameter. In this border domain we observe very long transients; precise identification of the dynamical states here requires a separate investigation.

Results for similar computations for a large range of ω are presented in Fig. 6. However, here the simulations were started from many different initial conditions. As one can see, partially synchronous states are characterized by a large degree of multistability: In fact, the whole range of SCPS is multistable, as can be seen in Fig. 6 as well as in Fig. 9 below. Different initial conditions result in different values of $\bar{\Omega}_r$ and $\bar{\nu}_r$ ⁶⁵. Interestingly, the variation of these quantities reduces with increasing ω . For all these parameters the mean fields of both populations remain synchronized; we have also checked that their phases remain well-defined⁶⁶.

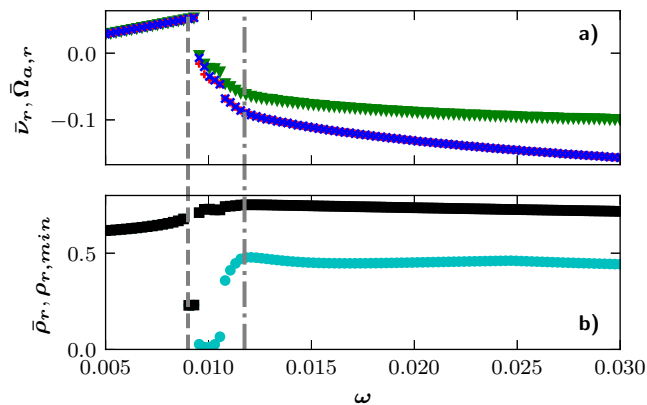


FIG. 5. a) Observed frequencies of oscillators from the repulsive group, $\bar{\nu}_r$ (green triangle), and of the mean fields $\bar{\Omega}_r$ (blue crosses) and $\bar{\Omega}_a$ (red pluses), for $N_a = N_r = 5$ and $\varepsilon = 0.212$. b) the average order parameter of the repulsive group $\bar{\rho}_r$ (black squares) and the minimal value of this order parameter over a long time interval, $\rho_{r,min} = \min_t[\rho_r(t)]$ (cyan circles). The analytical border of the solitary state is denoted by a dashed gray line; to the left of this line all frequencies coincide. Close to the border of the solitary state, the phase is not well defined, probably due to long transients, as indicated by low values of $\rho_{r,min}$. This leads to the discrepancies between $\bar{\Omega}_a$ and $\bar{\Omega}_r$. The right border of this domain is (quite arbitrary) marked by a dotted line. To the right of this border $\bar{\Omega}_r = \bar{\Omega}_a$ (blue crosses and red pluses overlap). The results have been obtained taking a perturbed cluster as initial condition.

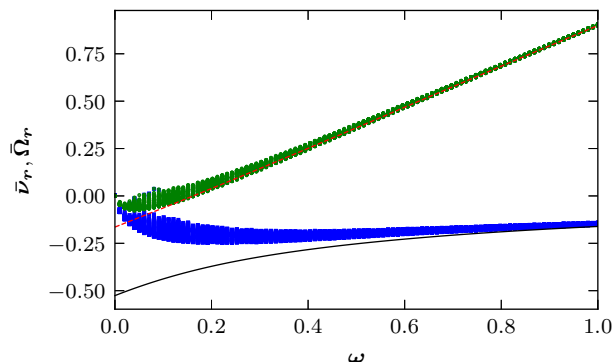


FIG. 6. The observed average frequency for $N_{a,r} = 5$ and $\varepsilon = 0.5$, for 100 random initial conditions per ω . The blue squares denote frequency $\bar{\Omega}_r$ of the mean field and the green dots denote frequency $\bar{\nu}_r$ of the repulsive oscillators. The dashed red line is the solution of Eq. (38) and the solid black line is the solution for the mean field frequency, see Eq. (34).

Notice that transition from the solitary state to partial synchrony is accompanied by change of the direction of rotation with respect to the considered coordinate frame⁶⁷. Indeed, before the transition all frequencies are positive, while immediately after it they are negative, see Fig. 5. With a further increase of the parameter ω , the frequency of the repulsive units $\bar{\nu}_r$ becomes positive and then tends to ω . In fact, for large ω or for strongly repulsive systems, the repulsive units tend to have a uniform distribution of phases. However, they remain perturbed by the field of the synchronous attractive cluster, so that the uniform distribution can be reached only asymptotically.

We illustrate partially synchronous dynamics of the repulsive group by several snapshots in Fig. 7, for an intermediate value $\omega = 0.1$. We see that repulsive oscillators form a group (a loose cluster), then the first oscillator in the group accelerates, stays for some instant in anti-phase with respect to others, so that we can speak about transient solitary state, and then joins the group again, now becoming the last one in the group. Then the group dissolves again, and now the oscillator that was initially the third in the group stays for some time in anti-phase to the rest of the group, then the group recombines, and so on. Notice that only every second oscillator undergoes the transient solitary state. This dynamics seem to be independent of the initial condition and was observed both for even and odd $N_{a,r}$. This bears some resemblance to a phenomenon observed in an ensemble of attractive and repulsive active rotators, see Ref.⁶⁸.

To conclude the discussion of the multistability of the partially synchronous state, we analyze a large system. In

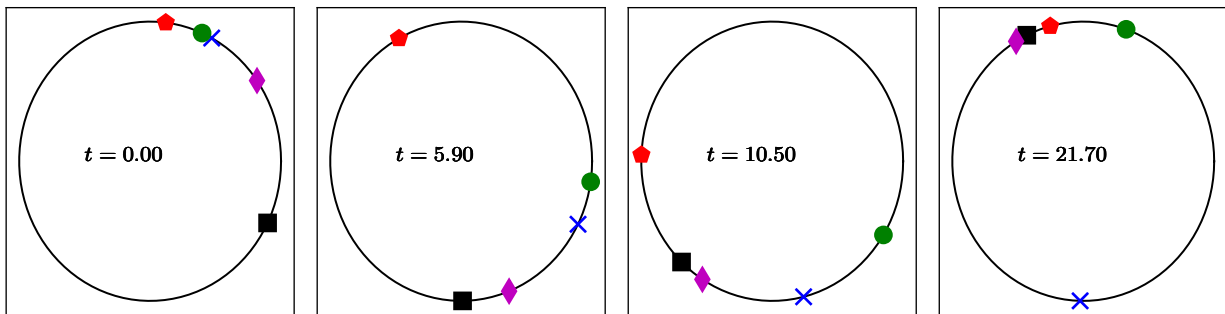


FIG. 7. A specific type of partial synchrony found in the system for intermediate values of ω . The snapshots shows the repulsive oscillators over time, where every oscillator is marked by a different color and symbol. At times $t = 5.9$ and $t = 21.7$ a single oscillator leaves the fuzzy cluster. The observed system is rather small with $N_r = N_a = 5$, $\varepsilon = 0.2$, and $\omega = 0.1$.

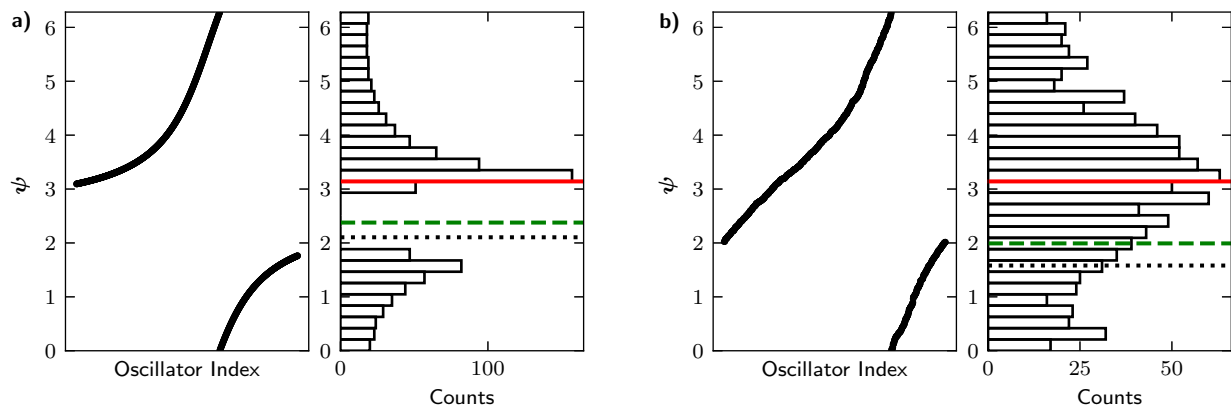


FIG. 8. Phases of the repulsive group and their histograms, for two different initial conditions and $N_{a,r} = 1024$, $\omega = 0.75$, and $\varepsilon = 0.5$. Initial conditions are perturbed cluster (a) and random (b). The solid red (dashed green) line is the phase of the repulsive (attractive) mean field Θ_r (Θ_a), while the dotted black line denotes the phase of the forcing Φ . The distribution in a) changes its width with time, whereas the distribution in b) is practically stationary.

Fig. 8 we show two distributions of phases ψ for $N_{a,r} = 1024$. These distributions have been obtained by simulation started from different initial conditions: in one case, illustrated in a), we use a perturbed cluster state, while the case in b) corresponds to random initial conditions. The distributions differ in their form, as well as in their dynamics. In the first case the distribution is bounded and bimodal; it moves with time and “breathes”, changing its width. Generally the phase differences between the mean fields and common force vary in time. In the case of random initial conditions phases spread around the unit circle and their distribution is unimodal and nearly stationary (small time fluctuations are probably due to finite size effect). The differences between the distributions also lead to slight differences in the average frequencies. For the perturbed cluster we find $\bar{\nu}_r = 0.262$ and $\bar{\Omega}_r = -0.196$ and for the random initial conditions we obtain $\bar{\nu}_r = 0.264$ and $\bar{\Omega}_r = -0.181$.

2. Theoretical analysis

Here we provide some analytical estimates for the state of partial synchrony. As already mentioned, for the case $\omega = 0$ and partial synchrony of the repulsive units, the relation between order parameters of two groups is given by Eq. (32). Since the attractive group is always synchronized, $\rho_a = 1$, we obtain $\rho_r = 1/(1 + \varepsilon)$. We expect that this expression can be used as an estimation also for small ω . We also expect that this expression yields the upper limit for ρ_r , since an increase in ω can only lead to a decrease in the level of synchrony.

Next, we recall that according to the WS theory the description of the system (4,5,6) can be reduced to six equations for collective variables. (Below we use the WS equations in the form, suggested in Ref.⁵⁶.) Furthermore, we restrict the consideration to the Ott-Antonsen (OA) manifold^{22,23} that corresponds to uniform distribution of the constants of motion in the WS theory⁵⁶. In this case the system is further simplified, with four equations for $\rho_{a,r}$ and $\Theta_{a,r}$.

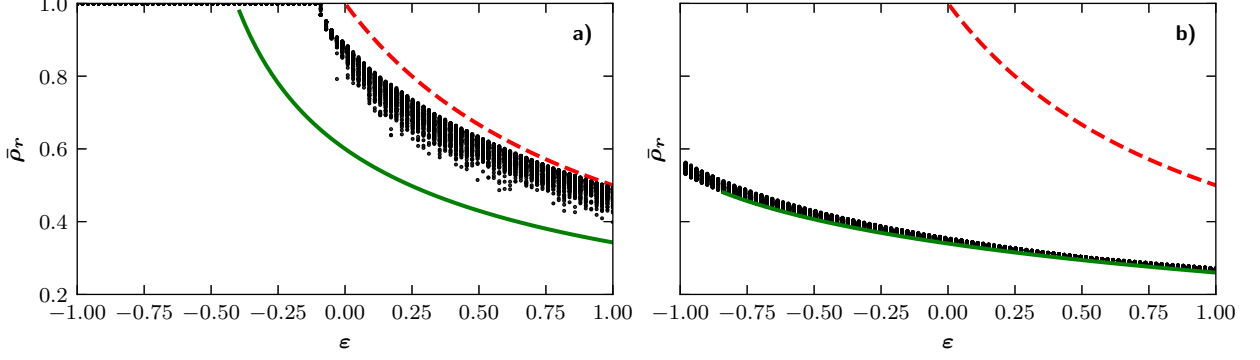


FIG. 9. The average repulsive order parameter $\bar{\rho}_r$ (black dots) for 100 different initial conditions per ε and $N_r = 5$. In a) $\omega = 0.02$ and in b) $\omega = 0.6$. The dashed red line marks $1/(1 + \varepsilon)$; as expected this curve yields a reasonable upper bound estimate for small ω . The solid green line the solution of Eq. (37); this estimation works better for large ω .

Moreover, since $\rho_a = 1$, we obtain a three-dimensional system. The final equations follow from the WS equations⁵⁶ and read

$$\dot{\rho}_r = \frac{1 - \rho_r^2}{4} [\cos(\Theta_r - \Theta_a) - (1 + \varepsilon)\rho_r] , \quad (33)$$

$$\dot{\Theta}_r = \omega + \frac{1 + \rho_r^2}{4\rho_r} \sin(\Theta_a - \Theta_r) , \quad (34)$$

$$\dot{\Theta}_a = \frac{1 + \varepsilon}{2} \rho_r \sin(\Theta_r - \Theta_a) . \quad (35)$$

Introduction of the phase shift between the mean fields $\delta = \Theta_r - \Theta_a$ leads to the two-dimensional system

$$\begin{aligned} \dot{\rho}_r &= \frac{1 - \rho_r^2}{4} [\cos \delta - (1 + \varepsilon)\rho_r] , \\ \dot{\delta} &= \omega - \frac{1 + [1 - 2(1 + \varepsilon)]\rho_r^2}{4\rho_r} \sin \delta . \end{aligned} \quad (36)$$

Notice that since we are very far from the thermodynamic limit, the OA Ansatz can be considered only as a rather crude approximation and, hence, Eqs. (36) provide only some estimates.

We are interested in states, where the mean fields are locked, and therefore δ is bounded. We consider a weaker condition $\dot{\delta} = 0$ and also neglect time variability of the order parameter, taking $\dot{\rho}_r = 0$. Applying this approximation to Eqs. (36) we obtain an estimation for the average order parameter $\bar{\rho}_r$:

$$\begin{aligned} \cos \delta &= (1 + \varepsilon)\bar{\rho}_r , \\ \sin \delta &= \frac{4\omega\bar{\rho}_r}{1 + (1 - 2(1 + \varepsilon))\bar{\rho}_r^2} . \end{aligned} \quad (37)$$

Eliminating δ by squaring the equations and reordering terms, we obtain a cubic equation for $\bar{\rho}_r^2$. The expression for the roots are too lengthy and therefore not shown; the results for the average order parameter $\bar{\rho}_r$ can be seen in Fig. 9. We see that for large ω the estimation of $\bar{\rho}_r$ is quite good.

Given $\bar{\rho}_r$ we find δ from Eqs. (37). In its turn, this yields the estimation of the average frequency of the repulsive mean field $\bar{\Omega}_r$ from Eq. (34) as $\bar{\Omega}_r = \omega + (1 + \bar{\rho}_r^2) \sin(\delta)/4\bar{\rho}_r$. For a known $\bar{\Omega}_r$ the average frequency of an oscillator can be calculated with the help of the WS theory⁶⁹. Using this we find the average frequency $\bar{\nu}_r$ of the repulsive oscillators (for the derivation see Appendix B) to be

$$\bar{\nu}_r = \frac{1 - \bar{\rho}_r^2}{1 + \bar{\rho}_r^2} \omega + \frac{2\bar{\rho}_r^2}{1 + \bar{\rho}_r^2} \bar{\Omega}_r . \quad (38)$$

The estimated $\bar{\nu}_r$ fits the numerical results in Fig. 6 for large ω quite well; the estimate $\bar{\Omega}_r$ is not as good, but also corresponds to the numerics for large ω .

V. CONCLUSION

We have analyzed the interplay of attraction and repulsion in a two-group Kuramoto model. In the considered network each group consists of identical elements but the groups differ in their frequencies. We have found that if attraction is stronger than repulsion then there exist an interval of frequency mismatch ω where the system synchronizes, in the sense that each group forms a cluster. The stronger the repulsion, the smaller is this interval of two cluster synchrony. The shift between synchronous clusters is determined by ω . A further increase of repulsion or of $|\omega|$ destroys the two-cluster synchrony. However, the attractive group remains synchronized while the repulsive one undergoes a transition to quasiperiodic partial synchrony. In this state the order parameter of the repulsive group is between zero and one, the mean field frequency remains locked to the frequency of the attractive group, but individual units have a different, generally incommensurate, frequency. For small $|\omega|$ the transition from two-cluster synchrony to partial synchrony occurs via formation of a solitary state. In this regime there exist two clusters (one with attractive units and one with all repulsive units but one) and one solitary repulsive oscillator. The borders of synchronous and solitary regimes have been obtained analytically. We notice that the domain of the solitary state solutions rapidly shrinks with the increase of ensemble size, whereas the partial synchrony persists for large ensembles as well. For large $|\omega|$ the frequencies of the individual units and of the mean field have been estimated with the help of the WS theory. We believe that our results can be useful for analysis of neuronal ensembles with excitatory and inhibitory connections.

ACKNOWLEDGMENTS

This paper was developed within the scope of the IRTG 1740 / TRP 2015/50122-0, funded by the DFG/ FAPESP. M. R. was supported by the Russian Science Foundation (Grant No. 17-12-01534). The authors thank A. Pikovsky and Y. Maistrenko for helpful discussions.

Appendix A: Stability of the Solitary State

The linear stability analysis of Eq. (30) with a perturbation of strength α yields

$$\dot{\delta}_{2\pm} = \delta_2 \pm \alpha = A[\sin(\delta_2 - \delta_2^* \pm \alpha) + \sin \delta_2^*]. \quad (\text{A1})$$

In the first order in α we find $\dot{\alpha} = -A \cos \delta_2^* \alpha$ and thus the condition for stability is $A \cos \delta_2^* > 0$. Since $A = \sin \delta_1 / (2 \sin \delta_2^*)$ this can also be written as

$$\frac{\sin \delta_1}{2 \tan \delta_2^*} > 0. \quad (\text{A2})$$

With the help of the definition of δ_2^* as $\tan \delta_2^* = \sin \delta_1 / ((1 + \varepsilon) - \cos \delta_1)$ the condition for stability becomes

$$1 + \varepsilon - \cos \delta_1 > 0. \quad (\text{A3})$$

Since the solitary states exists only for $\varepsilon > 0$, this condition is always fulfilled.

To demonstrate the stability of δ_1 is not that simple. The equation for δ_1 has the form

$$\dot{\delta}_1 = \sin \delta_1 \left[-\frac{1}{2} + \frac{1 + \varepsilon}{N} (N_r - 1) + \frac{1 + \varepsilon}{N} \cos \delta_2 \right] + \cos \delta_1 \frac{1 + \varepsilon}{N} \sin \delta_2 + \omega - \frac{1 + \varepsilon}{N} \sin \delta_2 \quad (\text{A4})$$

and cannot be reduced to a form similar to Eq. (30). So, we directly substitute he $\delta_{1\pm} = \delta_1 \pm \alpha$ and find

$$\dot{\alpha} = \alpha \left[\cos \delta_1 \left(-\frac{1}{2} + \frac{1 + \varepsilon}{N} (N_r - 1) + \frac{1 + \varepsilon}{N} \cos \delta_2 \right) - \sin \delta_1 \frac{1 + \varepsilon}{N} \sin \delta_2 \right]. \quad (\text{A5})$$

We analyze this equation numerically, by computing δ_1 and δ_2 with the help of Eq. (31); this analysis shows that δ_1 is also stable.

Appendix B: Oscillator frequency in the partially synchronous state

The WS theory operates with three collective variables; two of them are angles. The first one corresponds to the maximum of the distribution of individual phases. On the OA manifold this variable coincides with the phase of the mean field. The second angle variable (we denote it as χ) determines phase shift of individual oscillators with respect to the mean field (or, generally, outside of the OA manifold, with respect to the first angle variable). Correspondingly, the average frequency of units can be obtained as (see⁶⁹ for details):

$$\bar{\nu} = \bar{\Theta} - \bar{\chi}, \quad (\text{B1})$$

where Θ, χ obey the WS equations

$$\dot{\Theta} = \omega + \frac{1 + \rho^2}{2\rho} \text{Im}[He^{-i\Theta}], \quad (\text{B2})$$

$$\dot{\chi} = \frac{1 - \rho^2}{2\rho} \text{Im}[He^{-i\Theta}]. \quad (\text{B3})$$

Expressing $\bar{\chi}$ via $\bar{\Theta}$ we obtain the individual frequency

$$\bar{\nu} = \bar{\Theta} - \frac{1 - \rho^2}{1 + \rho^2} (\bar{\Theta} - \omega). \quad (\text{B4})$$

- ¹E. Kaempfer, *The history of Japan: together with a description of the kingdom of Siam, 1690-92*, Vol. 3 (AMS Press, 1906).
- ²S. H. Strogatz, D. M. Abrams, A. McRobie, B. Eckhardt, and E. Ott, "Theoretical mechanics: Crowd synchrony on the Millennium Bridge," *Nature* **438**, 43–44 (2005).
- ³E. A. Martens, S. Thutupalli, A. Fourrière, and O. Hallatschek, "Chimera states in mechanical oscillator networks," *Proceedings of the National Academy of Sciences* **110**, 10563–10567 (2013).
- ⁴S. Watanabe and S. H. Strogatz, "Constants of motion for superconducting Josephson arrays," *Physica D: Nonlinear Phenomena* **74**, 197 – 253 (1994).
- ⁵P. Richard, B. M. Bakker, B. Teusink, K. Dam, and H. V. Westerhoff, "Acetaldehyde mediates the synchronization of sustained glycolytic oscillations in populations of yeast cells," *European Journal of Biochemistry* **235**, 238–241 (1996).
- ⁶A. Prindle, P. Samayoa, I. Razinkov, T. Danino, L. S. Tsimring, and J. Hasty, "A sensing array of radically coupled genetic 'biopixels,'" *Nature* **481**, 39–44 (2011).
- ⁷D. Hansel, G. Mato, and C. Meunier, "Clustering and slow switching in globally coupled phase oscillators," *Physical Review E* **48**, 3470–3477 (1993).
- ⁸Y. Kuramoto and D. Battogtokh, "Coexistence of coherence and incoherence in nonlocally coupled phase oscillators." *Nonlinear Phenomena in Complex Systems* **5**, 380–385 (2002).
- ⁹V. Hakim and W.-J. Rappel, "Dynamics of the globally coupled complex Ginzburg-Landau equation," *Physical Review A* **46**, R7347–R7350 (1992).
- ¹⁰A. Hooper and R. Grimshaw, "Travelling wave solutions of the Kuramoto-Sivashinsky equation," *Wave Motion* **10**, 405–420 (1988).
- ¹¹C. Van Vreeswijk, "Partial synchronization in populations of pulse-coupled oscillators," *Phys. Rev. E* **54**, 5522 (1996).
- ¹²M. Rosenblum and A. Pikovsky, "Self-organized quasiperiodicity in oscillator ensembles with global nonlinear coupling," *Phys. Rev. Lett.* **98**, 064101 (2007).
- ¹³A. Pikovsky and M. Rosenblum, "Self-organized partially synchronous dynamics in populations of nonlinearly coupled oscillators," *Physica D: Nonlinear Phenomena* **238**, 27 – 37 (2009).
- ¹⁴P. Clusella, A. Politi, and M. Rosenblum, "A minimal model of self-consistent partial synchrony," *New Journal of Physics* **18**, 093037 (2016).
- ¹⁵Y. Maistrenko, B. Penkovsky, and M. Rosenblum, "Solitary state at the edge of synchrony in ensembles with attractive and repulsive interactions," *Phys. Rev. E* **89**, 060901 (2014).
- ¹⁶Y. Kuramoto, *Chemical oscillations, turbulence and waves* (Springer, Berlin, 1984).
- ¹⁷H. Sakaguchi and Y. Kuramoto, "A soluble active rotator model showing phase transitions via mutual entertainment," *Progress of Theoretical Physics* **76**, 576–581 (1986).
- ¹⁸J. A. Acebrón, L. L. Bonilla, C. J. P. Vicente, F. Ritort, and R. Spigler, "The Kuramoto model: A simple paradigm for synchronization phenomena," *Reviews of modern physics* **77**, 137 (2005).
- ¹⁹A. Pikovsky and M. Rosenblum, "Dynamics of globally coupled oscillators: Progress and perspectives," *Chaos: An Interdisciplinary Journal of Nonlinear Science* **25**, 097616 (2015).
- ²⁰D. Pazó, "Thermodynamic limit of the first-order phase transition in the Kuramoto model," *Physical Review E* **72** (2005), 10.1103/physreve.72.046211.
- ²¹S. Watanabe and S. H. Strogatz, "Integrability of a globally coupled oscillator array," *Phys. Rev. Lett.* **70**, 2391–2394 (1993).
- ²²E. Ott and T. M. Antonsen, "Low dimensional behavior of large systems of globally coupled oscillators," *Chaos: An Interdisciplinary Journal of Nonlinear Science* **18**, 037113 (2008).
- ²³E. Ott and T. M. Antonsen, "Long time evolution of phase oscillator systems," *Chaos: An Interdisciplinary Journal of Nonlinear Science* **19**, 023117 (2009).
- ²⁴M. Breakspear, S. Heitmann, and A. Daffertshofer, "Generative models of cortical oscillations: Neurobiological implications of the Kuramoto model," *Frontiers in Human Neuroscience* **4**, 190 (2010).

- ²⁵E. Montbrió, J. Kurths, and B. Blasius, “Synchronization of two interacting populations of oscillators,” *Phys. Rev. E* **70**, 056125 (2004).
- ²⁶D. M. Abrams, R. Mirollo, S. H. Strogatz, and D. A. Wiley, “Solvable model for chimera states of coupled oscillators,” *Physical review letters* **101**, 084103 (2008).
- ²⁷E. Barreto, B. Hunt, E. Ott, and P. So, “Synchronization in networks of networks: The onset of coherent collective behavior in systems of interacting populations of heterogeneous oscillators,” *Phys. Rev. E* **77**, 036107 (2008).
- ²⁸C. Van Vreeswijk, L. F. Abbott, and G. Bard Ermentrout, “When inhibition not excitation synchronizes neural firing,” *Journal of Computational Neuroscience* **1**, 313–321 (1994).
- ²⁹L. S. Tsimring, N. F. Rulkov, M. L. Larsen, and M. Gabbay, “Repulsive synchronization in an array of phase oscillators,” *Phys. Rev. Lett.* **95**, 014101 (2005).
- ³⁰A. V. Pimenova, D. S. Goldobin, M. Rosenblum, and A. Pikovsky, “Interplay of coupling and common noise at the transition to synchrony in oscillator populations,” *Scientific Reports* **6** (2016).
- ³¹H. Hong and S. H. Strogatz, “Kuramoto model of coupled oscillators with positive and negative coupling parameters: An example of conformist and contrarian oscillators,” *Phys. Rev. Lett.* **106**, 054102 (2011).
- ³²H. Hong and S. H. Strogatz, “Conformists and contrarians in a Kuramoto model with identical natural frequencies,” *Phys. Rev. E* **84**, 046202 (2011).
- ³³D. Anderson, A. Tenzer, G. Barlev, M. Girvan, T. M. Antonsen, and E. Ott, “Multiscale dynamics in communities of phase oscillators,” *Chaos: An Interdisciplinary Journal of Nonlinear Science* **22**, 013102 (2012).
- ³⁴D. Iatsenko, S. Petkoski, P. V. E. McClintock, and A. Stefanovska, “Stationary and traveling wave states of the Kuramoto model with an arbitrary distribution of frequencies and coupling strengths,” *Physical Review Letters* **110** (2013).
- ³⁵V. Vlasov, E. E. N. Macau, and A. Pikovsky, “Synchronization of oscillators in a Kuramoto-type model with generic coupling,” *Chaos: An Interdisciplinary Journal of Nonlinear Science* **24**, 023120 (2014).
- ³⁶T. Qiu, S. Boccaletti, I. Bonamassa, Y. Zou, J. Zhou, Z. Liu, and S. Guan, “Synchronization and bellerophon states in conformist and contrarian oscillators,” *Scientific reports* **6** (2016).
- ³⁷H. R. Wilson and J. D. Cowan, “Excitatory and inhibitory interactions in localized populations of model neurons,” *Biophysical Journal* **12**, 1 – 24 (1972).
- ³⁸C. Van Vreeswijk and H. Sompolinsky, “Chaos in neuronal networks with balanced excitatory and inhibitory activity,” *Science* **274**, 1724–1726 (1996).
- ³⁹A. Peyrache, N. Dehghani, E. N. Eskandar, J. R. Madsen, W. S. Anderson, J. A. Donoghue, L. R. Hochberg, E. Halgren, S. S. Cash, and A. Destexhe, “Spatiotemporal dynamics of neocortical excitation and inhibition during human sleep,” *Proceedings of the National Academy of Sciences* **109**, 1731–1736 (2012).
- ⁴⁰N. Dehghani, A. Peyrache, B. Telenczuk, M. L. V. Quyen, E. Halgren, S. S. Cash, N. G. Hatsopoulos, and A. Destexhe, “Dynamic balance of excitation and inhibition in human and monkey neocortex,” *Scientific Reports* **6** (2016).
- ⁴¹S. Brezetskyi, D. Dudkowski, and T. Kapitaniak, “Rare and hidden attractors in Van der Pol-Duffing oscillators,” *The European Physical Journal Special Topics* **224**, 1459–1467 (2015).
- ⁴²P. Jaros, Y. Maistrenko, and T. Kapitaniak, “Chimera states on the route from coherence to rotating waves,” *Physical Review E* **91** (2015), 10.1103/physreve.91.022907.
- ⁴³T. Chouzouris, I. Omelchenko, A. Zakharova, J. Hlinka, P. Jiruska, and E. Schll, “Chimera states in brain networks: Empirical neural vs. modular fractal connectivity,” *Chaos: An Interdisciplinary Journal of Nonlinear Science* **28**, 045112 (2018).
- ⁴⁴B. Chen, J. R. Engelbrecht, and R. Mirollo, “Dynamics of the Kuramoto-Sakaguchi oscillator network with asymmetric order parameter,” *Chaos: An Interdisciplinary Journal of Nonlinear Science* **29**, 013126 (2019).
- ⁴⁵S. Majhi, T. Kapitaniak, and D. Ghosh, “Solitary states in multiplex networks owing to competing interactions,” *Chaos: An Interdisciplinary Journal of Nonlinear Science* **29**, 013108 (2019).
- ⁴⁶T. Kapitaniak, P. Kuzma, J. Wojewoda, K. Czolczynski, and Y. Maistrenko, “Imperfect chimera states for coupled pendula,” *Scientific Reports* **4** (2014).
- ⁴⁷J. Hizanidis, N. Lazarides, G. Neofotistos, and G. Tsironis, “Chimera states and synchronization in magnetically driven SQUID metamaterials,” *The European Physical Journal Special Topics* **225**, 1231–1243 (2016).
- ⁴⁸E. Rybalova, N. Semenova, G. Strelkova, and V. Anishchenko, “Transition from complete synchronization to spatio-temporal chaos in coupled chaotic systems with nonhyperbolic and hyperbolic attractors,” *The European Physical Journal Special Topics* **226**, 1857–1866 (2017).
- ⁴⁹N. I. Semenova, E. V. Rybalova, G. I. Strelkova, and V. S. Anishchenko, “‘Coherence–incoherence’ transition in ensembles of nonlocally coupled chaotic oscillators with nonhyperbolic and hyperbolic attractors,” *Regular and Chaotic Dynamics* **22**, 148–162 (2017).
- ⁵⁰P. Jaros, S. Brezetsky, R. Levchenko, D. Dudkowski, T. Kapitaniak, and Y. Maistrenko, “Solitary states for coupled oscillators with inertia,” *Chaos: An Interdisciplinary Journal of Nonlinear Science* **28**, 011103 (2018).
- ⁵¹N. Semenova, T. Vadviasova, and V. Anishchenko, “Mechanism of solitary state appearance in an ensemble of nonlocally coupled Lozi maps,” *The European Physical Journal Special Topics* **227**, 1173–1183 (2018).
- ⁵²I. A. Shepelev, G. I. Strelkova, and V. S. Anishchenko, “Chimera states and intermittency in an ensemble of nonlocally coupled Lorenz systems,” *Chaos: An Interdisciplinary Journal of Nonlinear Science* **28**, 063119 (2018).
- ⁵³E. Rybalova, G. Strelkova, and V. Anishchenko, “Mechanism of realizing a solitary state chimera in a ring of nonlocally coupled chaotic maps,” *Chaos, Solitons & Fractals* **115**, 300–305 (2018).
- ⁵⁴M. Mikhaylenko, L. Ramlow, S. Jalan, and A. Zakharova, “Weak multiplexing in neural networks: Switching between chimera and solitary states,” *Chaos: An Interdisciplinary Journal of Nonlinear Science* **29**, 023122 (2019).
- ⁵⁵K. Sathiyadevi, V. K. Chandrasekar, D. V. Senthilkumar, and M. Lakshmanan, “Long-range interaction induced collective dynamical behaviors,” *Journal of Physics A: Mathematical and Theoretical* **52**, 184001 (2019).
- ⁵⁶A. Pikovsky and M. Rosenblum, “Partially integrable dynamics of hierarchical populations of coupled oscillators,” *Phys. Rev. Lett.* **101**, 264103 (2008).
- ⁵⁷A. Yeldesbay, A. Pikovsky, and M. Rosenblum, “Chimeralike states in an ensemble of globally coupled oscillators,” *Phys. Rev. Lett.* **112**, 144103 (2014).
- ⁵⁸R. Adler, “A study of locking phenomena in oscillators,” *Proceedings of the IRE* **34**, 351–357 (1946).
- ⁵⁹A. Pikovsky and M. Rosenblum, “Dynamics of heterogeneous oscillator ensembles in terms of collective variables,” *Physica D: Nonlinear Phenomena* **240**, 872–881 (2011).

- ⁶⁰S. A. Marvel, R. E. Mirollo, and S. H. Strogatz, “Identical phase oscillators with global sinusoidal coupling evolve by Möbius group action,” *Chaos: An Interdisciplinary Journal of Nonlinear Science* **19**, 043104 (2009).
- ⁶¹A. Pikovsky, “Private communication,”.
- ⁶²J. R. Engelbrecht and R. Mirollo, “Classification of attractors for systems of identical coupled Kuramoto oscillators,” *Chaos: An Interdisciplinary Journal of Nonlinear Science* **24**, 013114 (2014).
- ⁶³The attractive group remained fully synchronized even when the units were made non-identical by sampling the frequencies from a normal distribution with zero mean and standard deviation of 10^{-3} . Hence, stability of the attractive group is not a numerical artifact.
- ⁶⁴In the following the time-averaged quantities are denoted by overlined letters.
- ⁶⁵To obtain these quantities we have averaged the frequencies over the time interval of 500 units, after transient of 1000 units.
- ⁶⁶Even for such large values as $\omega = 1$ and $\varepsilon = 1$ the smallest observed order parameter over 100 different initial conditions was 0.08, with the average being 0.2.
- ⁶⁷We remind that we use the frame, co-rotating with the natural frequency of oscillators in the attractive group.
- ⁶⁸M. A. Zaks and P. Tomov, “Onset of time dependence in ensembles of excitable elements with global repulsive coupling,” *Phys. Rev. E* **93**, 020201 (2016).
- ⁶⁹Y. Baibolatov, M. Rosenblum, Z. Z. Zhanabaev, M. Kyzgarina, and A. Pikovsky, “Periodically forced ensemble of nonlinearly coupled oscillators: From partial to full synchrony,” *Phys. Rev. E* **80**, 046211 (2009).